A Tight-Binding Study of Acceptor Levels in Semiconductors

J. G. Menchero

Instituto de Física, Universidade Federal do Rio de Janeiro

Cx. Postal 68.528, 21945-970 Rio de Janeiro, Brazil

Received February 8, 1999

Acceptor binding energies in zinc-blende semiconductors are determined within the tight-binding formalism. The importance of fitting the valence-band masses in the (100) as well as (111) directions is discussed, and parametrizations that specifically fit the valence-band anisotropy are used to calculate Ge acceptor levels in $Al_xGa_{1-x}As$ alloys. The sensitivity of the calculated energies to the parameters that determine bulk masses is investigated, as well as the effect of varying the on-site energy of the impurity. A comparison is made between first-neighbor and second-neighbor hopping models. For shallow levels, both approaches give the same results. For deeper levels, however, important differences arise. Experimental evidence suggests that first-neighbor models are better suited for describing intermediate to deep levels.

I Introduction

The effective mass theory (EMT) has long been a principal tool for investigating shallow impurity states in semiconductors [1, 2]. In EMT, it is assumed that the impurity wave function is highly delocalized in real space, which in turn implies a strong localization in k space. As a result, the electronic properties of the host material may be described by only a few parameters related to the dispersion near the k point in consideration. For instance, in the Luttinger-Kohn version of $\mathbf{k} \cdot \mathbf{p}$ theory, the electronic structure of the host is completely defined in terms of the spin-orbit energy and the three Luttinger parameters (LP's), which also determine the impurity energy level. Because each host material has a different set of LP's, and acceptor binding energies are known to vary widely from host to host, it is clear that the impurity level within EMT must depend sensitively on these bulk parameters.

Another result of EMT is that, for a given material, any singly ionized acceptor should have the same binding energy, *regardless of the species*. However, experimentally it is known that such energies can vary widely from impurity to impurity. For example, an In acceptor in Si has a binding energy of 157 meV, compared to 45 meV for a B acceptor in the same host [3]. Such deviations from EMT are attributed to *central-cell effects*, and demonstrate that the binding energies can also be very sensitive to the details of the potential in the immediate neighborhood of the impurity.

Recently, an approach was presented [4] for calculating impurity states in semiconductors based on the tight-binding (TB) formalism. The localized basis set of TB provides a natural description for deep levels, while the highly delocalized shallow levels are treated by means of very large unit cells together with a scaling law that allows extrapolation to the bulk limit [4]. In other words, the TB approach is not intrinsically restricted to either the shallow or deep limits. For the TB approach to be useful, however, a clear understanding of how the calculated energies depend on the TB parameters is required. In particular, the sensitivity of EMT on the LP's and the the role of central-cell effects must be understood in the context of the current model. Another important question particular to TB concerns differences between first-nearest neighbor (1nn) and second-nearest neighbor (2nn) descriptions of the impurity state.

The aim of this paper is to carefully investigate how the impurity binding energies depend on the TB parameters that are most physically relevant to the impurity problem. The paper is organized as follows: In Sec. II the TB approach for calculating impurity states in semiconductors is briefly reviewed. In Sec. III the dependency of the impurity binding energy on the bulk

effective masses and the on-site energy of the impurity is investigated. Comparisons are also made between 1nn and 2nn TB approaches, with important differences found between the two. To illustrate these effects, Ge acceptors in GaAs, AlAs, and $Al_xGa_{1-x}As$ alloys are considered. The summary and conclusions are given in Sec. IV.

II Calculational Details

Our TB Hamiltonian contains terms describing the bulk material as well as the impurity, and is given by [4]

$$H = \sum_{ij}\sum_{\mu\nu} h^{ij}_{\mu\nu} c^{\dagger}_{i\mu} c_{j\nu} + \sum_{i}\sum_{\mu\nu} \lambda_i \langle \mu | l \cdot s | \nu \rangle \, c^{\dagger}_{i\mu} c_{i\nu} + \sum_{i}\sum_{\mu} U(r_i) c^{\dagger}_{i\mu} c_{i\mu} \ , \tag{1}$$

where the roman indices denote the site and the greek indices label the spin orbitals. The $h^{ij}_{\mu\nu}$ define all the on-site energies and hopping for the bulk material. In this work, both 1nn and 2nn hopping are considered. The strength of the spin-orbit interaction for atom i is defined by λ_i, and the on-site energy for atom i due to the Coulomb potential of the impurity is given by $U(r_i)$. For our basis set the sp^3s^* orbitals proposed by Vogl [5] is used, but spin is included here leading to a total of 10 basis states per site.

The perturbation potential $U(r_i)$ is described by an isotropic q-dependent screening,

$$U(r_i) = \frac{e^2}{\epsilon_0 r_i} + A\frac{e^2}{r_i} e^{-\alpha r_i} + (1-A)\frac{e^2}{r_i} e^{-\beta r_i} - \frac{e^2}{\epsilon_0 r_i} e^{-\gamma r_i} \ , \tag{2}$$

where the screening parameters A, α, β, and γ are taken from Bernholc [6]. Near the origin, the potential looks like a bare Coulomb potential $U_{\rm bare} = e^2/r_i$, but far away the potential looks like a bulk-screened potential $U_{\rm bulk} = e^2/\epsilon_0 r_i$, with ϵ_0 being the static dielectric constant for the host material. Precisely at the impurity site ($r_i = 0$), Eq. (2) is undefined and the perturbation potential is assigned a value U_0, where U_0 is a parameter describing central-cell effects.

In order to determine the acceptor energy, first the energy E_v at the top of the valence band is calculated for the pure system, setting $U(r_i) = 0$ for all i. This energy is easily found with the aid of Bloch's theorem. Next, a single impurity is placed in a very large cubic supercell containing $8L^3$ atoms arranged in the zinc-blende structure and subject to periodic boundary conditions, with L being the length of the supercell side in units of the conventional lattice parameter. The presence of the impurity breaks translational symmetry and introduces states in the gap region with energy above E_v. The energy $\tilde{E}_v(L)$ of the highest of these states determines the acceptor energy for supercell size L via the relation $E(L) = \tilde{E}_v(L) - E_v$. The main task therefore is to calculate $\tilde{E}_v(L)$, which is accomplished here using a variational algorithm that minimizes the expectation value of $\langle \Psi | (H - E_{ref})^2 | \Psi \rangle$, with E_{ref} being a reference energy suitably chosen near $\tilde{E}_v(L)$ [7]. The computation time using this scheme scales *linearly* with the number of states, making solutions possible even for very large supercells. For instance, system sizes ranging up to $L = 20$ (64000 atoms) are handled routinely [4]. However, using a recently proposed scaling law [4], the impurity binding energy can be extrapolated to the bulk limit using far smaller supercell sizes. In this scaling law, the energy $E(L)$ as a function of supercell size L is given by

$$E(L) = E_a + Pe^{-\alpha L} \ , \tag{3}$$

with E_a being the acceptor energy in the bulk limit ($L \to \infty$), and P being a constant independent of L. The acceptor energy for the infinite system can therefore be found by calculating $E(L)$ for three relatively small supercells and then solving for E_a, P, and α in

Eq. (3). When using Eq. (3) to find the binding energy in the bulk limit, caution must be exercised to verify not only that the supercell sizes are in the scaling regime, but also that the scaled energies have converged to the limiting value.

III Results

In EMT, the acceptor binding energy depends on the three Luttinger parameters γ_1, γ_2, and γ_3. These, in turn, can be related to the heavy-hole (HH) and light-hole (LH) masses along (100) and (111) [8],

$$\gamma_1 = \frac{1}{2}\left[m_{lh}^{-1}(100) + m_{hh}^{-1}(100)\right] , \quad (4)$$

$$\gamma_2 = \frac{1}{4}\left[m_{lh}^{-1}(100) - m_{hh}^{-1}(100)\right] , \quad (5)$$

$$\gamma_3 = \frac{1}{4}\left[m_{lh}^{-1}(111) - m_{hh}^{-1}(111)\right] , \quad (6)$$

where the masses in these expressions and throughout this work are in units of the free-electron mass. The fact that the LP's depend on the valence-band masses in both the (100) and (111) directions suggests that both are very important to fit properly in the TB parametrizations. On the other hand, due to the high density of states associated with the HH band, these masses are expected to be much more important than the LH masses for the purposes of determining the acceptor binding energies. Tight-binding parametrizations specifically chosen to fit the HH masses have been determined [9] both for 1nn and 2nn models, and will be used in this work. In Table 1 the valence-band masses resulting from these parametrizations are shown for GaAs and AlAs, together with the experimental [10] and theoretical [11] values.

The Ge acceptor in $Al_xGa_{1-x}As$ alloys acts as a simple substitutional impurity at the As site. The binding energy has been measured experimentally [12] using photoluminescence in the direct-gap range $0 < x < 0.4$, and the results are given by the dotted line in Fig.1. For pure GaAs, the binding energy is ~ 40 meV, but increases rapidly with an upward curvature to a relatively deep ~ 120 meV by $x = 0.40$. The binding energy curves $E_a(x)$ calculated using the 1nn and 2nn parametrizations are given in Fig.1 by the solid and broken lines, respectively. The VCA was used to obtain the Hamiltonian matrix elements for the alloy. Note, of course, that the VCA has no effect on the calculated binding energies at $x = 0$ or $x = 1$, which correspond to pure GaAs and pure AlAs respectively. The impurity perturbation potential U_0 was chosen in order that the calculated acceptor energy match the experimental value for pure GaAs. This led to a value of 3.42 eV for 2nn and 2.80 eV for 1nn. These values of U_0 were then used for all x, so that any variation in the acceptor energy with respect to x is attributable to the electronic response of the host material, and not to central-cell effects. The result for 2nn is in qualitative agreement with experiment, showing an increasing binding energy with increasing Al content. However, it significantly underestimates the binding energy at $x = 0.4$, with an energy of 71 meV compared to the experimental value of 120 meV. The result is improved considerably with 1nn, giving excellent agreement up to $x = 0.2$. However, the results diverge beyond that, and the binding energy of 87 meV at $x = 0.4$ is still substantially below the experimental value.

Table 1 - Heavy- and light-hole effective masses along [100] and [111], given in units of the free-electron mass.

Reference	Compound	$M_{HH}[100]$	$M_{LH}[100]$	$M_{HH}[111]$	$M_{LH}[111]$
Experiment [a]	GaAs	0.340	0.094	0.750	0.082
2nn (this work)	GaAs	0.346	0.074	0.751	0.066
1nn (this work)	GaAs	0.374	0.070	0.750	0.064
Theory [b]	AlAs	0.413	0.183	1.136	0.143
2nn (this work)	AlAs	0.416	0.178	1.137	0.140
1nn (this work)	AlAs	0.605	0.134	1.136	0.122

[a] Reference 10

[b] Reference 11

In order to investigate the possibility that small uncertainties in the effective masses for AlAs might produce better agreement with experiment, the sensitivity of the binding energy to the HH masses is studied. The HH masses for AlAs are scaled by a factor $\tilde{m}$ ranging from 0.60 and 1.40 in such a way as to not modify any of the band energies at Γ [9]. Even though scaling the HH masses by such a large fraction may have an

adverse effect on some conduction-band features, these are of little importance in determining acceptor binding energies. In the inset of Fig.1, the acceptor energy at $x = 0.4$ is plotted as a function of $\tilde{m}$, for both 1nn and 2nn cases. A remarkably linear behavior is observed over a wide range of HH masses. Interestingly, the 1nn model is much more sensitive to variations in the HH mass, with even a modest increase greatly improving agreement with experiment. For the 2nn model, however, even increasing the HH mass by 40% leads to binding energy of only 93 meV, compared to 120 meV in experiment. It is worthwhile here to comment that in order to obtain good agreement with experiment (say 110 meV at $x = 0.4$) a binding energy of ~ 400 meV is required for $x = 1.0$ (i.e., pure AlAs). This energy serves as a useful reference for the analysis considered below.

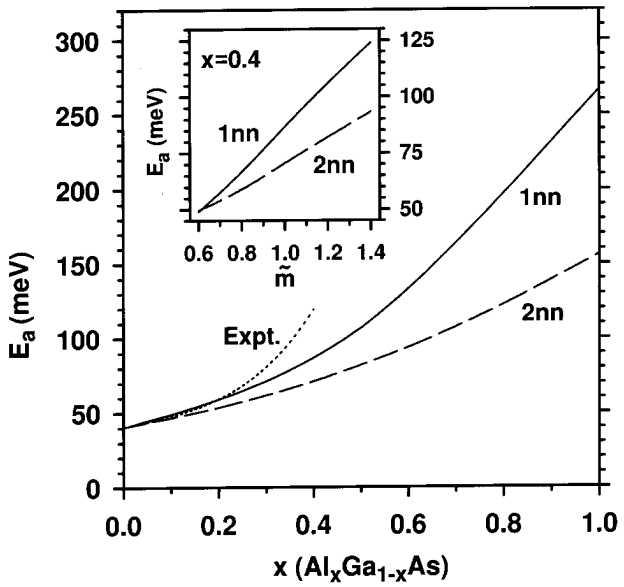

Figure 1. Acceptor energies E_a for Ge impurities in $Al_xGa_{1-x}As$ alloys, calculated with 1nn (solid line) and 2nn parametrizations (dashed line). The experimental result is given by the dotted line. Inset: acceptor energy at $x = 0.4$ as a function of the mass scaling factor $\tilde{m}$ for 1nn and 2nn parametrizations.

Varying the TB parameters that determine the HH masses in effect changes the *bulk* properties of the host. However, it is also possible to vary the TB parameters that pertain only to the *impurity*, without modifying the bulk properties. These parameters would therefore describe central-cell effects, and can be incorporated within the present theory through the on-site energy U_0 of the impurity itself. Up to now, it has been assumed that U_0 was independent of the host. Nevertheless, it is instructive to consider what effect variations in U_0 have on the impurity energies. In Fig.2(a) the acceptor energy calculated for a range of U_0 is presented for GaAs and AlAs using the 2nn parametrizations. The curves are characterized by three distinct regimes: an energetically flat regime for small U_0, a linearly increasing regime for large U_0, and a transition region for intermediate U_0. In the flat region, different impurity species (characterized by different U_0) will have nearly identical binding energies, meaning that central-cell corrections will be very small. Such behavior is typical of shallow levels, which implies that EMT is expected to work well in this regime.

It is interesting to note that in going from GaAs to AlAs (i.e., increasing HH mass), the energetically flat regime gets pushed to ever smaller U_0. In fact, for AlAs, the flat region is never quite reached, except perhaps for $U_0 < 1$ eV using 2nn, and so central-cell corrections are expected to always be important for this host. It should also be kept in mind that the Coulomb potential due to the impurity as given by Eq. (2) is roughly 0.6 eV at the nearest-neighbor distance (2.45 Å). Therefore, it is unphysical to consider acceptors with U_0 smaller than this value. The linear regime observed for large U_0 marks the breakdown of the effective mass approach. In EMT, the impurity potential is assumed to be slowly varying on the atomic length scale. A potential of say 5.0 eV at the impurity site, falling to 0.6 eV at the nearest neighbor, clearly violates this approximation. In the linear regime, central-cell effects are expected to be very important, because even small variations in U_0 (due to different impurities) will lead to large changes in binding energy.

In Fig.2(b) the impurity energy is plotted as a function of U_0 for AlAs and GaAs using the 1nn parametrization. Qualitatively, the results are similar to the 2nn case shown in Fig. (a). However, the 1nn case is once again found to be far more sensitive than the 2nn case. For instance, increasing U_0 to just 3.3 eV is sufficient to give a binding energy of 400 meV in AlAs with 1nn, whereas a value of 5.5 eV is required with a 2nn model. Recalling that for GaAs the value of U_0 was 3.42 eV for 2nn and 2.80 eV for 1nn, and considering the chemical similarity between GaAs and AlAs, a value of 5.5 eV seems unrealistic. Therefore, the interpretation once more is that the 1nn results are more consisitent with experiment.

In order to obtain a better understanding of the connection between 1nn and 2nn models, it is necessary to compare the two cases directly, using the same value of U_0. According to EMT, the acceptor binding

energy should depend only on the effective masses near the k point under consideration. From this point of view, no difference should exist between 1nn and 2nn parametrizations, *as long as the effective masses were the same*. In order to quantitatively study the validity of this assertion, however, the 1nn and 2nn TB parameters must be adjusted so as to give the same HH masses in the (100) as well as (111) directions [9]. Next, a value of U_0 sufficiently small (0.7 eV) is chosen so that the EMT should be expected to hold, and the binding energy calculated as a function of x, where as usual x is the Al concentration of the $Al_xGa_{1-x}As$ alloy. The results are plotted in Fig.3, and show that the 1nn and 2nn results are in *almost exact agreement over the entire range of* x. This is reassuring, because for shallow levels the energy can only depend on the effective mass if the TB result is to be consisitent with EMT. The second case to be considered is for larger U_0, in which the EMT can be expected to break down. A value of $U_0 = 3.5$ eV is used and the energy $E_a(x)$ recalculated. From Fig.3, a radical difference is now observed between 1nn and 2nn parametrizations. For GaAs, the 1nn result gives 70 meV compared with only 42 meV using 2nn. In passing, it is instructive to note that the EMT result breaks down strongly for the $U_0 = 3.5$ eV case in GaAs but not for the $U_0 = 0.7$ eV case in AlAs, even though the binding energies are comparable. This demonstrates that binding energy considerations alone are not enough to determine if a level can or cannot be described by EMT. In any case, the breakdown of EMT is even more dramatic for the $U_0 = 3.5$ eV case in pure AlAs, with the 1nn approach yielding an energy of 454 meV compared with 182 meV using 2nn. The experimental data suggest, therefore, that *1nn descriptions are more appropriate than 2nn for the case of deep levels*. The likely reason is that the 2nn hopping terms permit the electron to escape more easily from the impurity potential, thereby delocalizing the wave function and reducing the binding energy. To confirm this conjecture, the radial charge distribution is calculated for an AlAs host using both 1nn and 2nn with an on-site energy U_0 of 3.5 eV. It is found indeed that the electron is far more delocalized using the 2nn approach. For instance, using 1nn, there is a 90% probability of localizing the electron within 7 Å of the impurity, whereas using the 2nn parametrization, the same probability is reached at roughly 14 Å.

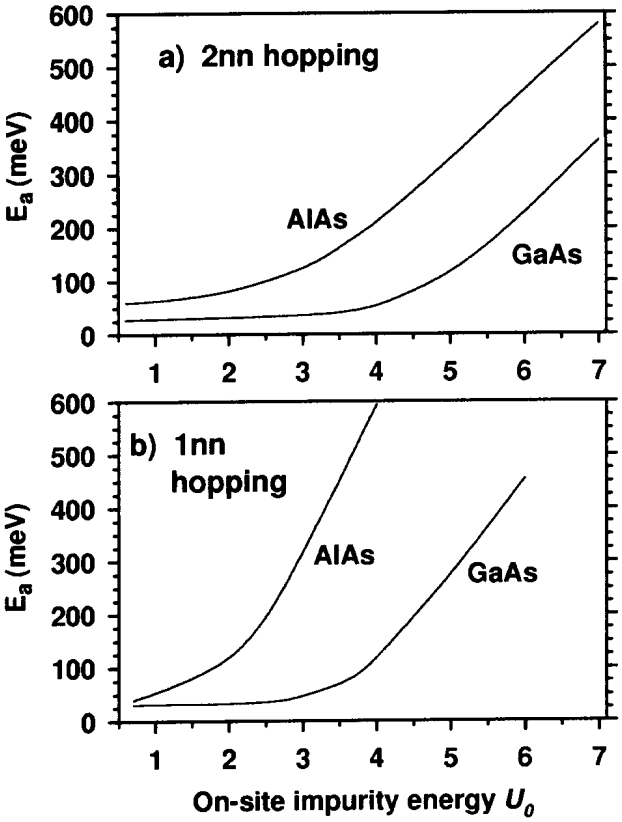

Figure 2. Acceptor binding energies for Ge impurities as a function of the on-site impurity potential U_0 (a) Using 2nn parametrization for AlAs and GaAs. (b) Using 1nn parametrization for AlAs and GaAs. The flat region for small U_0 indicates the regime in which EMT is expected to work well.

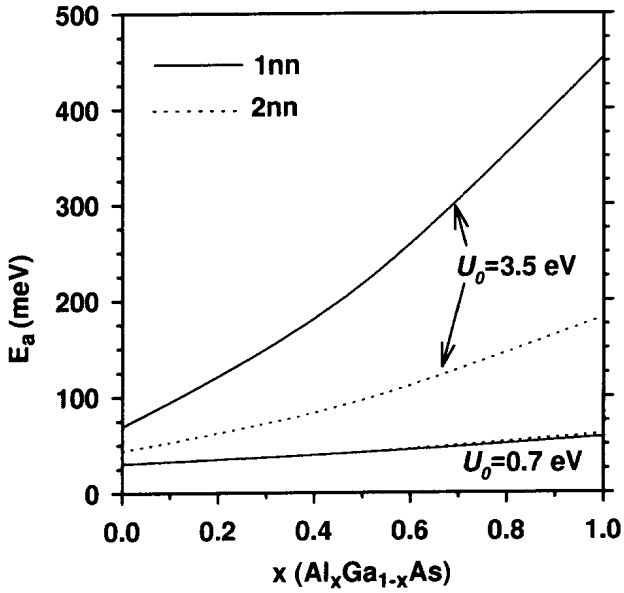

Figure 3. Acceptor energies calculated for shallow levels ($U_0 = 0.7$ eV) and deep levels ($U_0 = 3.5$ eV) using 1nn (solid line) and 2nn (dotted line) parametrizations, with the same HH effective masses. The $U_0 = 0.7$ results are consistent with EMT, whereas major deviations are observed for $U_0 = 3.5$.

IV Summary and Conclusions

Binding energies have been calculated for acceptors in GaAs, AlAs, and $Al_xGa_{1-x}As$ hosts. It was found that the 1nn model is much more sensitive than the 2nn model to small changes in the parameters. Insight was gained into why and when central-cell corrections become important. For shallow levels in which central-cell corrections are unimportant, the 1nn and 2nn models give the same results. However, for intermediate to deep levels, the two results deviate, and experimental evidence suggests that the 1nn model is more appropriate. The reason is that the 2nn model is not as effective in binding the wave function to the impurity. The 2nn parametrizations are expected to be most useful therefore for describing shallow levels, due to their superior ability to fit the effective masses. A particularly interesting application of the 2nn approach may be for the case of donors in indirect gap materials, due to intrinsic limitations in the 1nn ability to fit conduction- band dispersion near the zone boundary.

Acknowledgements

Helpful discussions with Belita Koiller, Rodrigo Capaz, Helio Chacham, and Timothy Boykin are gratefully acknowledged. The financial support of CNPq, PRONEX, and FINEP is also greatly appreciated.

References

[1] C. Kittel and A. H. Mitchell, Phys. Rev. **96**, 1488 (1954).

[2] J. M. Luttinger, and W. Kohn, Phys. Rev. **97**, 869 (1955).

[3] C. Kittel, *Introduction to Solid State Physics, 7th Ed.*, (Wiley, 1996) p. 225.

[4] J. G. Menchero, R. B. Capaz, Belita Koiller, and H. Chacham, Phys. Rev. B **59**, 2722 (1999).

[5] P. Vogl, H. P. Hjalmarson, and J. D. Dow, J. Phys. Chem. Solids **44**, 365 (1983).

[6] J. Bernholc and S. T. Pantelides, Phys. Rev. B **15**, 4935 (1977).

[7] J. K. L. MacDonald, Phys. Rev. **46**, 828 (1934); R. B. Capaz, G. C. de Araujo, Belita Koiller, and J. P. von der Weid, J. Appl. Phys. **74** 5531 (1993); L. W. Wang and A. Zunger, J. Chem. Phys. **100**, 2394 (1994).

[8] R. Enderlein, G. M. Sipahi, L. M. R. Scolfaro, and J. R. Leite, Phys. Stat. Sol. (b) **206**, 623 (1998).

[9] J. G. Menchero and T. B. Boykin, *Impurity states in semiconductors calculated via tight-binding: a parameter sensitivity study*, Phys. Rev. B **59**, *to appear* (1999).

[10] R. V. Shanabrook, O. J. Glembocki, D. A. Broido, and W. I. Wang, Phys. Rev. B **39**, 3411 (1989).

[11] L. Pavesi and M. Guzzi, J. Appl. Phys. **75**, 4779 (1994).

[12] G. Oelgart, B. Lippold, R. Heilmann, H. Neumann, and B. Jacobs, Phys. Stat. Sol. A **115**, 257 (1989).